

# Hybrid effects on tensile properties of hybrid short-glass-fiber-and short-carbon-fiber-reinforced polypropylene composites

SHAO-YUN FU\*

*Advanced Materials Research Centre, Nanyang Technological University,  
Nanyang Avenue, Singapore 639798  
E-mail: assyfu@ntu.edu.sg*

BERND LAUKE, EDITH MÄDER

*Institut fuer Polymerforschung Dresden e. V., Hohe Strasse 6, D-01069 Dresden, Germany*

CHEE-YOON YUE, XIAO HU

*Advanced Materials Research Centre, Nanyang Technological University,  
Nanyang Avenue, Singapore 639798*

YIU-WING MAI

*Centre for Advanced Materials Technology, Department of Mechanical & Mechatronic Engineering, The University of Sydney, N. S. W. 2006, Australia*

Hybrid composites of polypropylene reinforced with short glass fibers and short carbon fibers were prepared using extrusion compounding and injection molding techniques. The tensile properties of these composites were investigated taking into account the effect of the hybridization by these two types of short fibers. It was noted that the tensile strength and modulus of the hybrid composites increase while the failure strain of the hybrid composites decreases with increasing the relative carbon fiber volume fraction in the mixture. The hybrid effects for the tensile strength and modulus were studied by the rule of hybrid mixtures (RoHM) using the tensile strength and modulus of single-fiber composites, respectively. It was observed that the strength shows a positive deviation from that predicted by the RoHM and hence exhibits a positive hybrid effect. However, the values of the tensile modulus are close to those predicted by the RoHM and thus the modulus shows no existence of a hybrid effect. Moreover, the failure strains of the hybrid composites were found to be higher than the failure strain of the single carbon fiber-reinforced composite, indicating that a positive hybrid effect exists. Explanations for the hybrid effects on the tensile strength and failure strain were finally presented.

© 2001 Kluwer Academic Publishers

## 1. Introduction

Hybridization with more than one type of fibers used in a single matrix leads to the development of hybrid fiber composites. In principle several different types of fiber can be incorporated into a hybrid system but in practice it is likely that a combination of only two types of fibers would be most useful [1]. Carbon and glass fibers are often used in the same polymeric resin matrix to form hybrids. Carbon fiber provides a strong, stiff and low density reinforcement but is relatively expensive and brittle, while glass fiber is relatively cheap and has better fracture property but its strength and stiffness are relatively low. By hybridization, it is possible to design the material to better suit various requirements. At the same time, material costs can be substantially re-

duced by a careful selection of reinforcing fibers. By combining the two fibers with the same matrix, it is possible to achieve a balance between the properties of all-carbon fiber reinforced plastics and all-glass fiber reinforced plastics. For example, by combining carbon fibers and glass fibers a reduction in modulus might be acceptably traded for increased fracture resistance and failure strain, and reduced cost for the hybrid composite when compared with the single-carbon fiber reinforced composite. On the contrary, a reduction in fracture resistance would be traded for increased modulus and strength when compared with the single-glass fiber reinforced composite.

A certain mechanical property, such as strength or modulus of a hybrid system consisting of two single

\* Present Address: Centre for Advanced Materials Technology, Department of Mechanical & Mechatronic Engineering, The University of Sydney, N. S. W. 2006, Australia.

systems, can be predicted by the rule of hybrid mixtures (RoHM)

$$P_H = P_G V_G + P_C V_C \quad (1)$$

where  $P_H$  is the property to be investigated,  $P_G$  the corresponding property of the first system such as glass fiber/polypropylene and  $P_C$  the corresponding property of the second system such as carbon fiber/polypropylene.  $V_G$  and  $V_C$  are, respectively, the relative hybrid volume fraction of the first system and the second system, and  $V_G + V_C = 1$ . A positive or negative hybrid effect is defined as a positive or negative deviation of a certain mechanical property from the rule of hybrid mixtures behavior. The results on the mechanical properties of hybrid laminates reinforced with glass and carbon fibers have been discussed extensively [1–10]. The principal properties such as tensile [2], flexural [4], compression [6] strength, tensile elastic modulus [1, 2, 4, 7], stress intensity [2] and fracture toughness [2] were observed to show no signs of a hybrid effect. Namely, these properties of the hybrid composite laminates are simply a weighted sum of the corresponding properties of the individual components. Nonetheless, the properties of hybrid composites might not always follow a direct consideration of the independent properties of the individual components and would show possible positive or negative hybrid effects. For example, the fracture energy of hybrid glass/carbon/epoxy composites was observed to show a negative hybrid effect [2, 7]. The compression modulus of hybrid glass and carbon reinforced composites was reported to exhibit a negative hybrid effect [6]. A review of the literature on carbon fiber and glass fiber hybrid reinforced plastics indicated that incorporation of both fibers into a single matrix sometimes leads to better properties than would be expected from consideration of the rule of mixtures [3]. The tensile modulus of glass-rich hybrids [7, 8] and the flexural modulus of sandwich hybrid beam [4] were found to show a positive hybrid effect. Also, in glass/carbon-reinforced polymer systems, a positive hybrid effect for the strain was calculated and presented in Table I of the reference [7]. And a positive hybrid effect (i.e. failure strain enhancement) in flexural tests on sandwich coupons with a high glass mat to carbon fiber content ratio was observed as well [4]. Here the so-called hybrid effect on strains is the enhancement of the (initial or ultimate) failure strain of the low elongation-fiber-reinforced, non-hybrid composite [5, 7, 9]. Zweben [10] reported on hybrid composites containing low (carbon) and high (glass) elongation fibers to interpret this positive hybrid effect. He concluded that on failure of the hybrid composites, high elongation fibers in the composite enhance the strain level required to propagate

cracks through the composites and hence high elongation fibers behave like crack arrestors on a micromechanical level. However, all these previous studies have been concentrated on systems in which reinforcements are oriented continuous fibers. Very limited work has been carried out on hybrid short-glass-fiber and short-carbon-fiber reinforced composites [11–13]. Miwa and Horiba [11, 12] investigated the effects of fiber length and strain rate on tensile strength of epoxy resin reinforced with random-planar orientation of short carbon and glass fibers. They showed that (1) the tensile strength of the hybrid composites increased as the length of the reinforcing fibers increased and remained almost unchanged after the fiber length reached a certain level, this is consistent with the theoretical result [14]; and (2) the tensile strength increased as the strain rate increased. Moreover, it was shown that the tensile strength of the hybrid composites could be estimated by the rule of hybrid mixtures using the tensile strength of both single composites, indicating that no hybrid effect on the tensile strength was observed. Creep behavior of a hybrid glass/carbon-reinforced composite has been studied [13]. Short glass fiber and short carbon fiber were mechanically mixed in accordance with the designed volume fraction ratio 1 : 1. Hybrid effects were not involved.

Short-fiber-reinforced polymer (SFRP) composites are often made with conventional techniques, namely extrusion compounding and injection molding, for processing polymers [15–24]. During processing of SFRP compounds, fiber breakage takes place. One of the major factors influencing fiber breakage is fiber-fiber interaction [25]. When the volume fraction ratio of the two types of fibers in the hybrid is varied, the interaction between these fibers leads to changes in their fiber lengths [22]. It is generally accepted that the properties of hybrid composites are controlled not only by properties of components and fiber-matrix interface but also by fiber length and hybrid design etc. Moreover, a requisite for the occurrence of a hybrid effect is that the two types of fibers will differ by both their mechanical properties and by the interfaces they form with the matrix [2].

In the present study, the question of hybrid effects will be examined with short glass fiber (SGF)/short carbon fiber (SCF) hybrids on tensile properties of injection molded hybrid polypropylene (PP) composites. Hybrid polypropylene composites reinforced with short glass fibers and short carbon fibers were prepared with extrusion compounding and injection molding techniques. We studied the effect of the hybridization by SGF and SCF on tensile properties of the hybrid SGF/SCF/PP composites. The hybrid effects were studied on the tensile strength, tensile modulus and failure strain of the hybrid composites. Since the mechanical properties of glass and carbon fibers and the interfacial properties of GF/PP and CF/PP systems differ greatly, the hybrid effects would very likely exist for their hybrid reinforced composites. The hybrid effects have been calculated using the rule of hybrid mixtures for the tensile strength and modulus. The tensile strength shows the existence of a positive hybrid effect but the tensile modulus exhibits no sign of a hybrid effect. Moreover, fracture strain results show that the

TABLE I Mechanical and physical properties of materials at 23 °C

Materials	Tensile strength (MPa)	Young's modulus (GPa)	Density (kg/m <sup>3</sup> )	Diameter (μm)
Glass fiber	1956*	78.51*	2550	13.8
Carbon fiber	3950*	238*	1770	7.5
Polypropylene	31.6	1.30	903	

\*Test length = 50 mm.

failure strain of the hybrid composites is higher than that of the short-carbon-fiber-reinforced polypropylene composite, hence the failure strain exhibits a positive hybrid effect.

## 2. Experimental details

### 2.1. Materials

The materials employed in this investigation were polypropylene (HOSTALEN PPN 1060 + 2 wt.-% POLYBOND 3150), E-glass fiber roving (EC 14-300-E 37 300 tex) and carbon fiber roving (TENAX HTA 5331, 800 tex). The mechanical and physical properties of these materials are listed in Table I. The total fiber volume fraction is fixed at 25% for the hybrid SGF/SCF/PP system. The hybrid three-component system can be considered to consist of the SGF/PP system and the SCF/PP system and both the single-fiber systems have a fiber volume fraction of 25%. The glass fiber volume fraction  $V_f$  (GF) and the carbon fiber volume fraction  $V_f$  (CF) are respectively (25%, 0%), (18.75%, 6.25%), (12.5%, 12.5%), (6.25%, 18.75%) and (0%, 25%). The relative carbon fiber volume fraction is then 0%, 25%, 50%, 75% and 100%. In other words, the volume ratio of the SCF/PP system to the whole hybrid system is 0%, 25%, 50%, 75% and 100%.

### 2.2. Specimen preparation

The composites were prepared by feeding the glass and carbon fiber roving into the polymer melt using a twin-screw extruder. The six heating zones were set to 230, 230, 220, 220, 220 and 220°C and the mass temperatures were 214, 231, 239, 236, 233 and 231°C. The compounded extrudates were immediately quenched in water and cooled in air to ambient temperature. Then the extruded strands were chopped into granules and dried. All the specimens were injection molded into dumbbell-shaped tensile bars under identical conditions using a twin-screw injection molding machine with a barrel temperature of 210 to 230°C. An end-gated mold was used according to DIN 53455. The fibers in the tensile bars were preferentially oriented in the flow direction [20, 23, 26, 27]. This is shown in Fig. 1.

### 2.3. Tensile tests

The tensile properties of specimens were determined using 10 samples for each composition with a Zwick 1456 testing machine at a constant cross-speed of 5 mm/min.

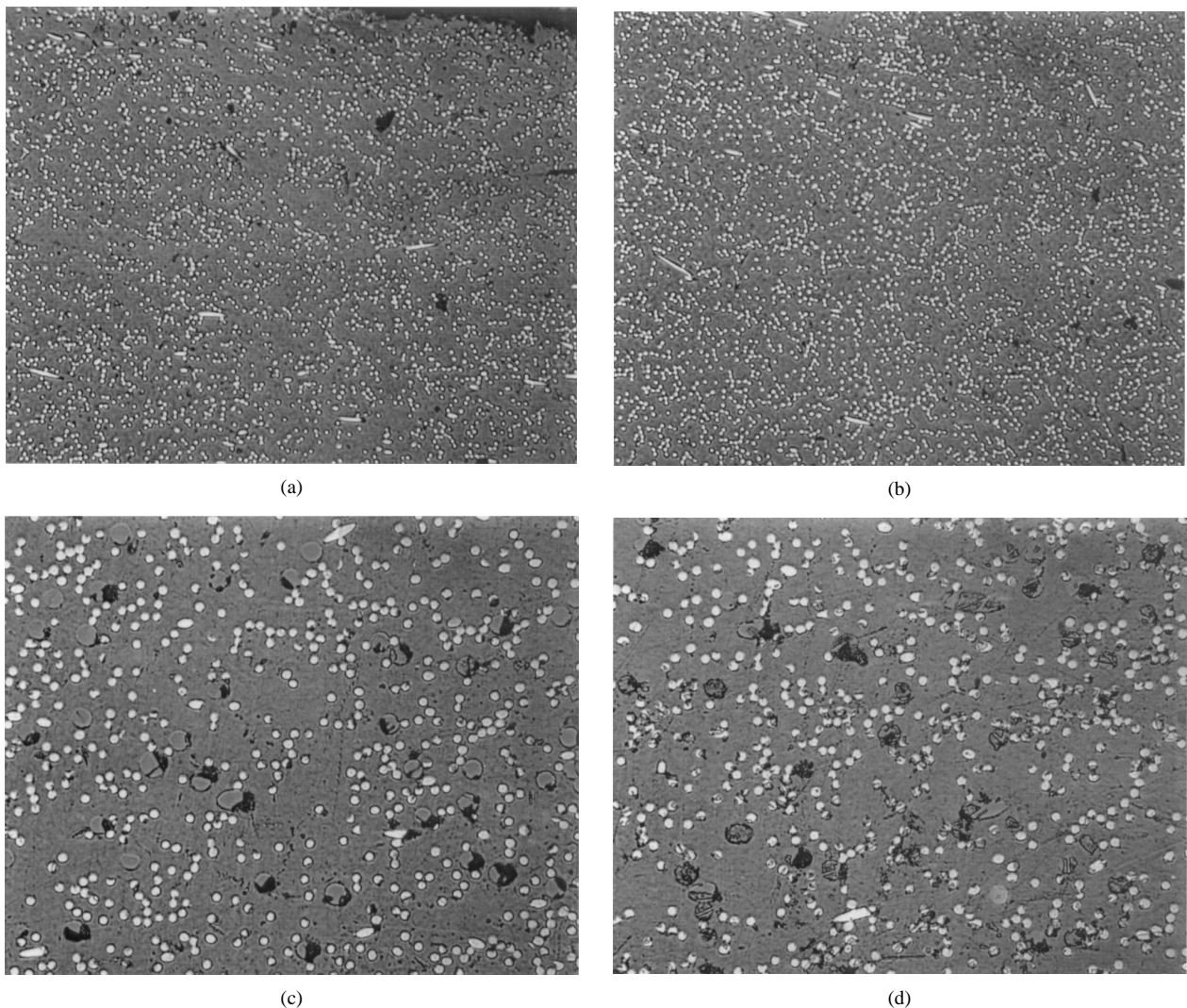


Figure 1 Orientation of fibers in specimens taken from: (a) the side and (b) the central area of the SCF/PP composite with  $V_f$  (carbon) = 25%, (c) the side and (d) the central area of the hybrid SGF/SCF/PP composite with  $V_f$  (carbon) = 18.75% and  $V_f$  (glass) = 6.25%.

## 2.4. Measurement of fiber length and orientation

Short glass and carbon fibers were first isolated from the composite materials by pyrolysis in a microwave oven for about ten minutes at 550 °C. An ash of fibrous material was left and some fibers were extracted from the sample ash and dispersed in water in a rectangular glass dish. The dish was then placed on the observation stage of a microscope. Magnified fiber images were transmitted to a large screen, and fiber images were then semi-automatically digitized by software with a computer and fiber length distributions (FLD) were thus determined. Fiber orientation was measured with an optical reflected-light microscopy from polished sections of the materials perpendicular to the specimen axis.

## 2.5. SEM observations

Prior to scanning electron microscopy (SEM) observations, all fracture surfaces of the tensile specimens were sputter-coated with gold. Fractographic studies with SEM were carried out in detail on the fracture surfaces of the hybrid SGF/SCF/PP composites.

## 2.6. Measurement of mean interfacial shear stress at the maximum fiber pull-out force of glass fiber/polypropylene and carbon fiber/polypropylene samples

Single-glass-fiber/polypropylene and single-carbon-fiber/polypropylene model composites were prepared for single-fiber pull-out tests. A self-made pull-out apparatus [28] has been used to measure fiber displacement and force. The fibers were embedded in the matrix at 230°C under argon atmosphere. The embedded fiber lengths were from 150 to 300 μm. The pull-out tests were carried out under the same velocity (0.2 μm/s) of pulling out the fibers at ambient temperature. The fiber diameter  $d_f$  was measured microscopically. From each

force-displacement curve the maximum force  $F_{max}$  was determined. The maximum force is determined by the interfacial debonding and friction between fiber and matrix and the geometry of the sample. The shear stress distribution along the interface is not homogeneous [29, 30]. Hence, an interpretation of the maximum force ( $F_{max}$ ) normalized by the surface area ( $\pi d_f l_e$ , where  $l_e$  is the embedded fiber length) as interfacial shear strength characterizing adhesion is inappropriate [31]. However, in this study, we define the mean interfacial shear stress  $\hat{\tau}$  at the maximum fiber pull-out load as:

$$\hat{\tau} = \frac{F_{max}}{\pi d_f l_e} \quad (2)$$

The mean values of  $\hat{\tau}$  for the two single-fiber polymer systems were estimated from 15 to 20 pull-out tests.  $\hat{\tau}$  provides only a mean value (at the point of maximum applied load) of the strongly inhomogeneous shear stress distribution and cannot be expected to be a physical measure for interfacial adhesion in the sense of a material property. But it can be taken as a measure for load transmission ability from a fiber to matrix for comparison of different material combinations or can be used as an approximation in evaluation of critical fiber length.

## 3. Results and discussion

### 3.1. Fiber length and orientation

The effect of the relative carbon fiber volume fraction on the mean glass and carbon fiber lengths is presented in Table II and Fig. 2, where the total glass and carbon volume fraction is fixed at 25%. It is of interest to note that the mean glass and carbon fiber lengths decrease with the increase of relative carbon fiber volume fraction and the decrease of relative glass fiber volume fraction. This indicates that the glass to carbon fiber interaction brings about more damage to the glass fibers than the glass-glass interaction while the same fiber

TABLE II Distributional data on the fiber length profile (1001 to 1005 fibers)

Length classes (μm)	Relative frequency for fiber concentrations spanned								
	$V_f$ (GF) = 25% $V_f$ (CF) = 0%		$V_f$ (GF) = 18.75% $V_f$ (CF) = 6.25%		$V_f$ (GF) = 12.5% $V_f$ (CF) = 12.5%		$V_f$ (GF) = 6.25% $V_f$ (CF) = 18.75%		$V_f$ (GF) = 0% $V_f$ (CF) = 25%
	GF	GF	CF	GF	CF	GF	CF	CF	
0–44	0	0	0	0	0	0	0	0	0
44–62	0	0	0	0	0	0	0	0.002	0.002
62–88	0	0	0.008	0	0.003	0	0.006	0.009	0.009
88–125	0	0	0.0259	0	0.016	0	0.0677	0.0726	0.0726
125–176	0	0	0.1127	0.0060	0.1176	0.0109	0.1821	0.2100	0.2100
176–250	0.0179	0.045	0.2373	0.0398	0.3041	0.0507	0.3473	0.3144	0.3144
250–353	0.0906	0.1548	0.3210	0.1841	0.3539	0.2199	0.2388	0.2617	0.2617
353–500	0.2998	0.3736	0.2173	0.4010	0.1755	0.4259	0.1333	0.0915	0.0915
500–707	0.3665	0.3536	0.0668	0.3184	0.0299	0.2577	0.0169	0.0348	0.0348
707–999	0.1922	0.0729	0.011	0.0478	0	0.0328	0.006	0.004	0.004
999–1414	0.0289	0	0	0.003	0	0.002	0	0	0
1414–1999	0.003	0	0	0	0	0	0	0	0
1999–2828	0.001	0	0	0	0	0	0	0	0
Mean fiber length (μm)	586.54	491.25	310.02	472.40	284.00	446.33	253.30	249.44	

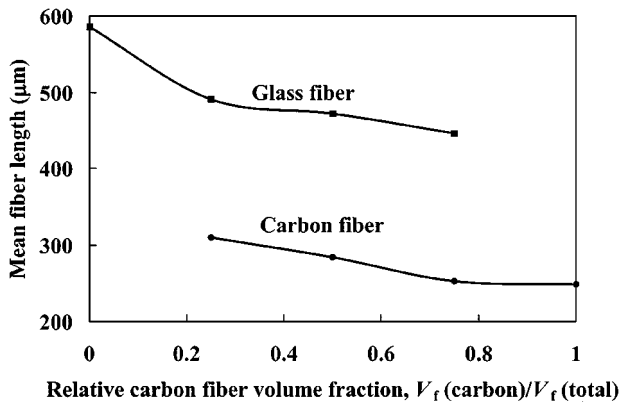


Figure 2 Number-average glass and carbon fiber lengths for hybrid SGF/SCF/PP composites.

interaction leads to less damage to the carbon fibers than the carbon-carbon interaction [22].

The critical fiber length ( $l_c$ ) can be evaluated with the following formula:

$$l_c = \frac{r_f \sigma_{fu}}{\hat{\tau}} \quad (3)$$

where  $\sigma_{fu}$  is the fiber strength and  $r_f$  is the fiber radius. This relation is valid if it is assumed that the interface shear stress is constant along the axis of a fiber embedded in a representative volume element. Then, we can use, as an approximation, the values of  $\hat{\tau}$  determined by the pull-out experiments to evaluate  $l_c$ . The measured mean values of  $\hat{\tau}$  for glass/PP and carbon/PP systems from 15–20 single fiber pull-out tests are, respectively, 15.2 MPa and 18.2 MPa. Thus, the critical lengths of glass fibers and carbon fibers can be obtained as 887.92  $\mu\text{m}$  and 813.87  $\mu\text{m}$ , respectively. The glass and carbon fiber length distributions presented in Fig. 3 show that the fiber length distributions for both glass and carbon fibers shift towards the left side [except it is not very clear between  $V_f(\text{carbon}) = 18.25\%$  and  $V_f(\text{carbon}) = 25\%$ ] as the relative carbon fiber volume fraction increases. This indicates that more damage to both fibers is brought out as the relative carbon fiber volume fraction increases. Moreover, Fig. 3 and Table II show that most glass fibers have a length less than their critical length and nearly all carbon fibers are much shorter than their critical length. So, most fibers would be pulled out instead of fracture during loading of the composite, this will be shown in Fig. 5b.

The orientation of fibers is optically observed on polished sections of specimens and is shown in Fig. 1, where the optical micrographs are selected arbitrarily but are typical ones. For both single and hybrid composites, the fibers are preferentially aligned along the flow direction (i.e. the normal direction of the polished sections of the specimens). For short single-fiber composites, this has also been observed previously [20, 23, 26, 27].

### 3.2. Tensile stress-strain curves

Tensile stress-strain curves of hybrid SGF/SCF/PP composites are shown in Fig. 4. The hybrid com-

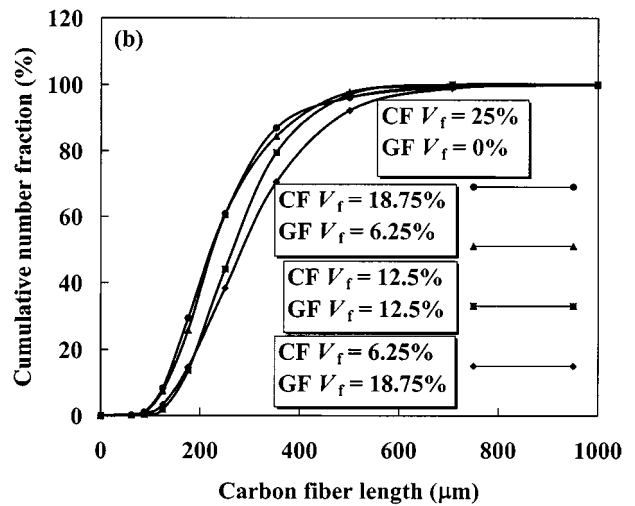
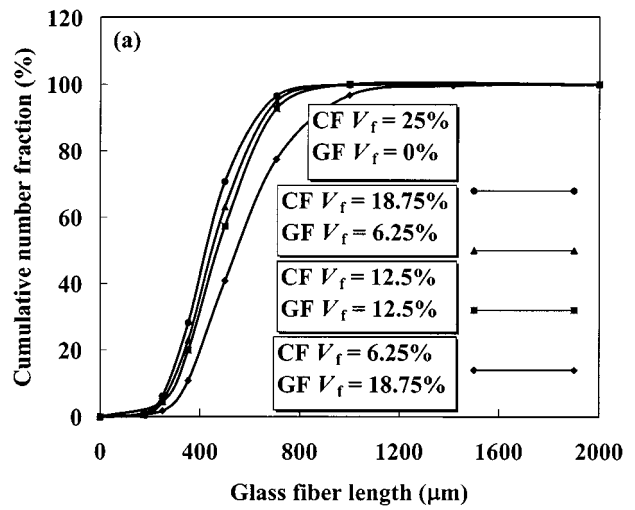


Figure 3 (a) Glass and (b) carbon fiber length distributions for hybrid SGF/SCF/PP composites.

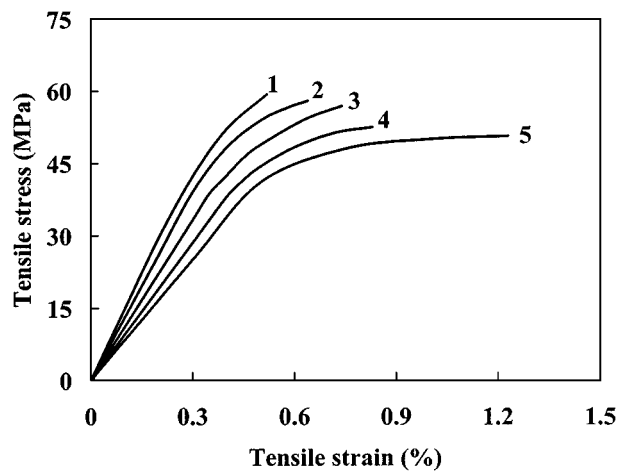


Figure 4 Typical tensile stress-strain curves for hybrid SGF/SCF/PP composites. Curve 1: 25 vol % carbon fibers; curve 2: 6.25 vol % glass fibers and 18.75 vol % carbon fibers; curve 3: 12.5 vol % glass fibers and 12.5 vol % carbon fibers; curve 4: 18.75 vol % glass fibers and 6.25 vol % carbon fibers; curve 5: 25 vol % glass fibers.

posites exhibit brittle fracture and show linear deformation at low stress and non-linear deformation at high stress. This non-linear deformation behavior indicates that (1) interfacial micro-failure at the fiber

ends occurs in the composites, (2) the micro-failure propagates along the fiber lengths, (3) plastic deformation bands of the matrix take place, (4) crack opening occurs in the band and the crack grows slowly through the band [32]. Finally, a catastrophic crack propagation takes place through the matrix pulling out fibers from the matrix [32]. The curves shift from the right side to the left side as the relative carbon fiber volume fraction increases. This is due to the fact that the modulus of carbon fiber is higher than that of glass fiber and thus the composite modulus increases with the increase of relative carbon fiber volume fraction. Moreover, the failure strain for the hybrid composites decreases with increasing relative carbon fiber volume fraction. This may be partially attributed to the more brittle nature of the carbon fiber compared to glass fiber. Furthermore, as the relative carbon fiber volume fraction increases, the composite strength increases. The increase in the ultimate strength of composites is at least partially due to the high strength of the carbon fiber.

### 3.3. Fractography

Fig. 5 represents the SEM micrographs of the fracture surfaces of a hybrid SGF/SCF/PP composite. The brittle

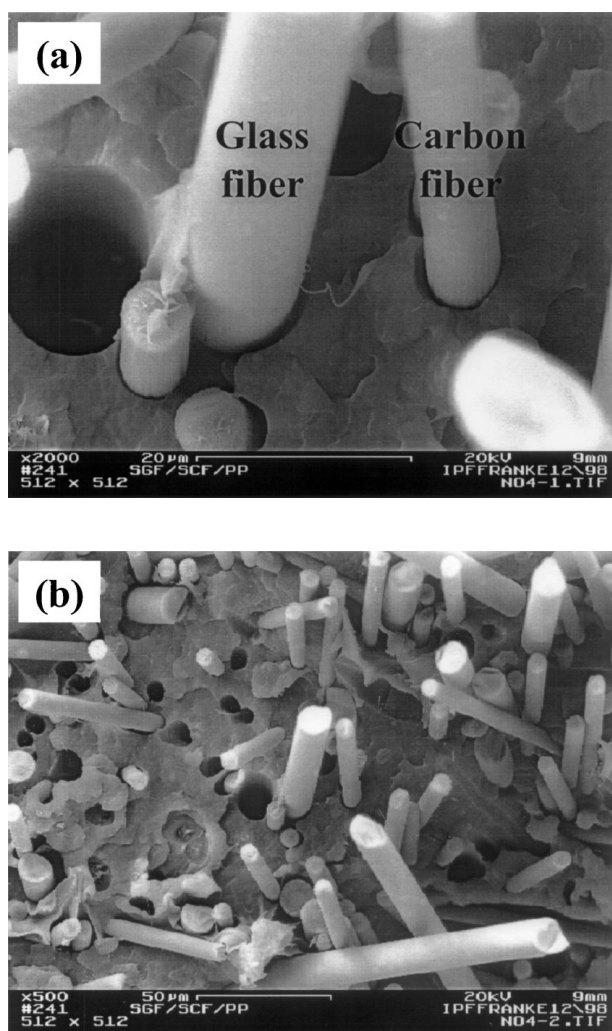


Figure 5 SEM micrographs of tensile fracture surfaces of a hybrid SGF/SCF/PP composite with a carbon fiber volume fraction of 12.5% or a relative carbon fiber volume fraction of 50%: (a)  $\times 2000$ , (b)  $\times 500$ .

fracture of the matrix can be clearly seen in the hybrid composite (Fig. 5a). Short glass fibers and short carbon fibers are intimately mixed in the matrix (Fig. 5b), glass and carbon fibers can be easily distinguished by their different diameter. Moreover, Fig. 5b shows that most of glass fibers and carbon fibers are pulled out (see the pulled out fibers and the pull-out holes). This is because most of the fibers (see Fig. 3) are shorter than the measured critical fiber lengths ( $l_c = 887.92 \mu\text{m}$  for glass fibers and  $813.87 \mu\text{m}$  for carbon fibers).

### 3.4. Tensile properties

Fig. 6 shows the results about the strength of the hybrid SGF/SCF/PP composites. The ultimate strength is significantly improved by the incorporation of glass and carbon fibers. This strength improvement is found to increase with increasing relative carbon fiber volume fraction. Since the fibers are preferentially aligned along the flow direction (i.e. the applied loading direction) for injection molded tensile specimens (see Fig. 1), the fiber orientation can be roughly assumed unchanged with the relative fiber volume fraction. When the relative carbon fiber volume fraction is increased, the mean glass and carbon fiber lengths decrease (see Table II and Fig. 2). When the changes in fiber lengths are considered, the strength of the hybrid composites can be predicted using the RoHM (Equation 1) and the existing theory (Equations 4 and 5 to be presented later) for the strength of short fiber-reinforced composites [14]. As an approximation, the values of the mean interfacial shear stress obtained from single fiber pull-out tests are used. The predicted values of the strength of the hybrid composites are presented in Fig. 6. It can be seen that the experimental values of the ultimate strength of the hybrid fiber composites lie above the “mixtures rule” prediction. This indicates that the strength exhibits a positive deviation from the mixture rule (i.e. the RoHM prediction) and hence shows a positive hybrid effect. It has been shown that the interfacial shear stress at short fiber ends would have the maximum value [33]. Since the carbon fiber has a higher stiffness than the glass fiber and the mean aspect ratios of carbon fibers are much smaller than those of

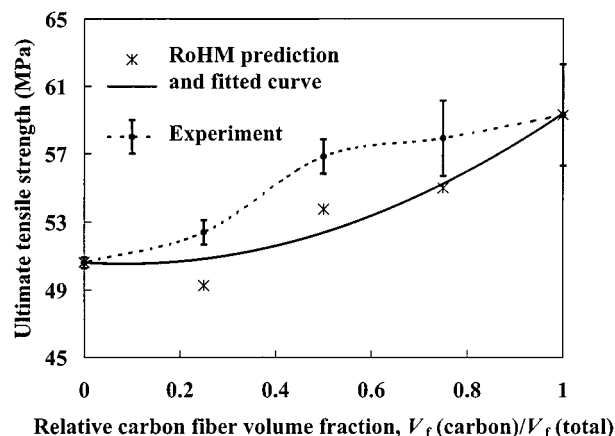


Figure 6 Ultimate strength versus relative carbon fiber volume fraction for hybrid SGF/SCF/PP composites.

glass fibers, according to the stress transfer theory [33] the shear stress at the carbon fiber ends would have the higher maximum value. Since  $\tau_s$  for the glass-PP and carbon-PP system are of the same magnitude, interfacial debonding would hence take place first at the carbon fiber ends. Thus, micro-cracks would also start there. Namely, carbon fibers represent sources of defects that would cause cracks. As the applied tensile strain or load is increased, the cracks propagate along the carbon fiber length and also across the neighboring matrix. In the presence of glass fibers, the cracks would be “bridged” by these fibers, allowing the carbon fibers to have a larger contribution to the tensile strength of the hybrid composites than to the single carbon fiber reinforced composite. Consequently, a positive hybrid effect on the strength of hybrid composites has been observed. Schematic illustrations of the failure processes of composites (Figs 9 and 10) and quantitative estimation (Fig. 11) of the hybrid effect will be presented later.

Fig. 7 shows the results for the modulus of the hybrid SGF/SCF/PP composites. It can be seen that the modulus of the hybrid composites is greatly enhanced by the addition of both short glass and carbon fibers (the matrix modulus is 1.3 GPa). Moreover, the composite modulus increases with increasing relative carbon fiber volume fraction. The modulus of the hybrid composites is predicted using the rule of hybrid mixtures and existing theories for the modulus of short fiber composites [34, 35]. The predicted values are presented in Fig. 7, which shows that the experimental values of the modulus of the hybrid composites are close to the predicted values, indicating that the modulus exhibits no hybrid effect.

Fig. 8 shows the effect of the relative carbon fiber volume fraction on the failure strain of the hybrid SGF/SCF/PP composites. The failure strain decreases with increasing relative carbon fiber volume fraction but is higher than that of the single-carbon-fiber-reinforced composite. This is due to the fact that the propagation of the cracks at the carbon fiber ends would be arrested when they reach the glass fibers. This would result in a higher failure strain of the hybrid composites than that of the single carbon fiber composite. It is also noted that the failure strain of the hybrid composites

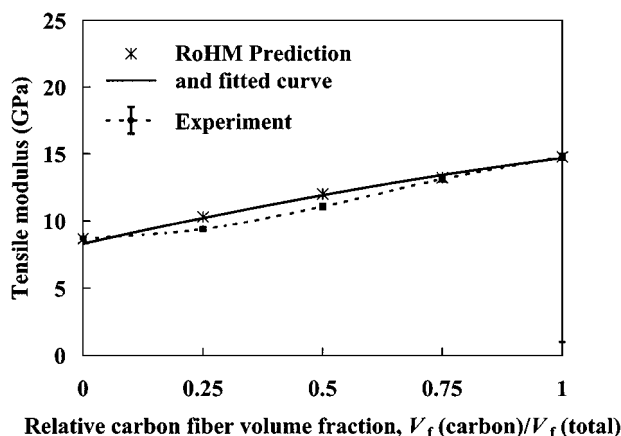


Figure 7 Tensile modulus versus relative carbon fiber volume fraction for hybrid SGF/SCF/PP composites.

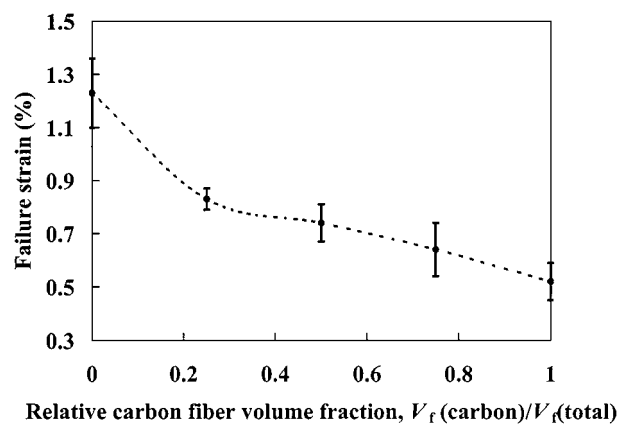


Figure 8 Failure strain versus relative carbon fiber volume fraction for hybrid SGF/SCF/PP composites.

is lower than that of the single-glass-fiber-reinforced composite. This is because as the cracks propagate across the matrix and approach the glass fibers, the glass fibers adjacent to the cracks are subjected to a strain concentration [10], this would lead to a lower failure strain of the hybrid composites than that of the single glass fiber composite. In addition, the positive hybrid effect for the strain has been defined as an increase in the maximum strain at failure, when compared to the strain of the two-phase composite containing the stiffer fiber [7, 9]. So, Fig. 8 shows a positive hybrid effect on the failure strain of the hybrid composites. Existing studies [27, 32, 36] on failure mechanisms show that under tensile stress, the cracks start at the fiber ends and propagate along the fiber-matrix interface or across the matrix and finally failure takes place. Thus, this positive hybrid effect implies that the cracks started at carbon fiber ends do not lead to failure of the hybrid composites because the glass fibers act as crack arrestors. Schematic illustration of the hybrid effect is shown in Fig. 10.

The failure processes of short fiber reinforced polymer composites have been studied previously [27, 32]. Schematic illustration of the fracture of short carbon fiber composites is presented in Fig. 9. As the applied strain is increased to  $\varepsilon_1$ , the microcracks take place at the carbon fiber ends (Step 1). Then, the cracks propagate along fiber length (Step 2). And the cracks spread across the matrix (Step 3). When the cracks grow to a critical size, catastrophic crack propagation occurs and final fracture of the composite takes place (Step 4). However, when part of carbon fibers is replaced by glass fibers, the failure processes would be different as shown in Fig. 10. As the applied strain is increased to  $\varepsilon_1$ , cracks would start at carbon fiber ends (see Step 1 of Fig. 10). When the applied strain is increased to  $\varepsilon_2$ , the cracks would propagate along the carbon fiber length, and microcracks would also occur at glass fiber ends (see Step 2). As the applied strain is further increased to  $\varepsilon_4$ , the cracks initiated at carbon fiber ends would run through the matrix and reach the glass fibers. These cracks would be “bridged” by the glass fibers; and in the meantime, the cracks caused by the glass fibers would propagate along glass fiber lengths (see Step 3). The cracks caused by the carbon fibers do not

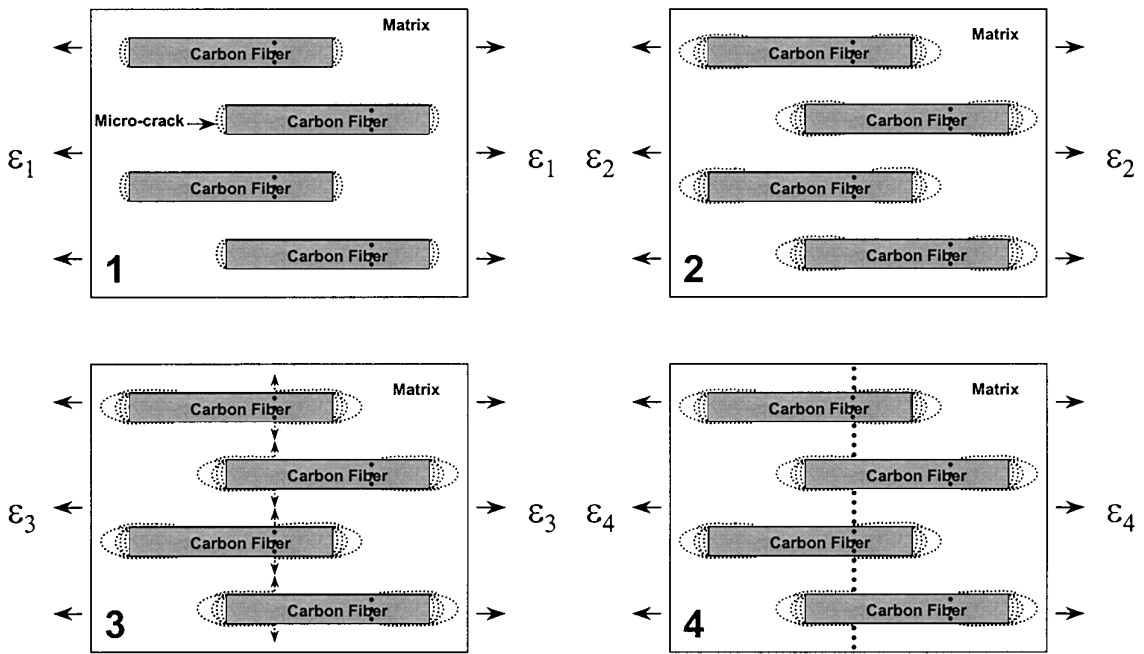


Figure 9 Schematic drawing of microfailure processes of single short (carbon) fiber-reinforced polymer composites.

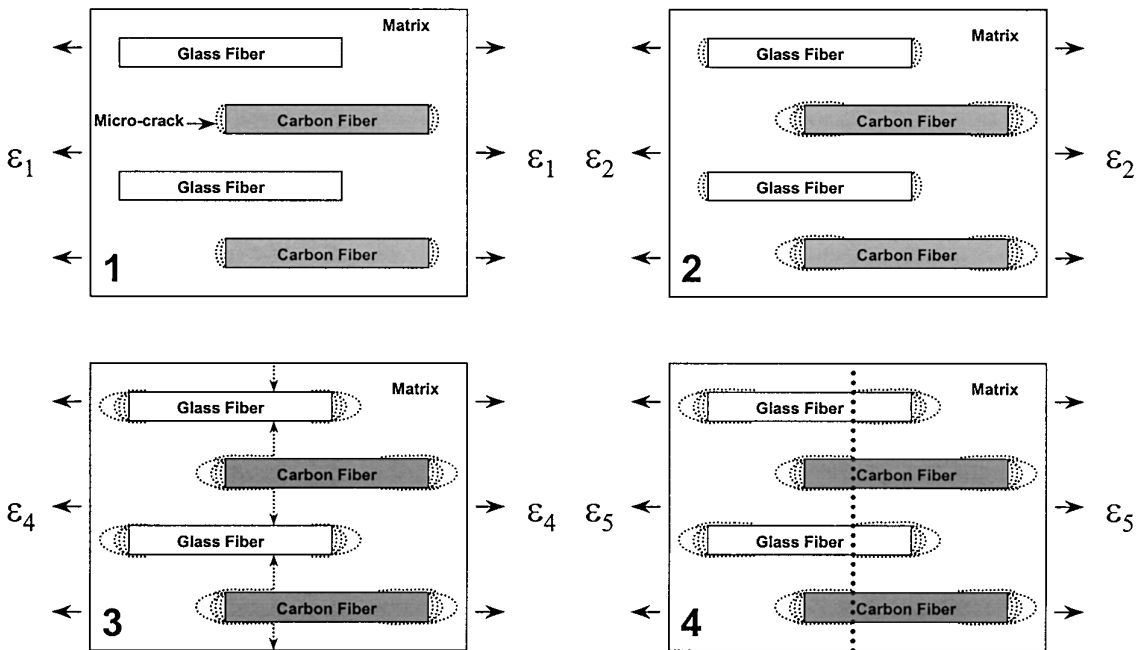


Figure 10 Schematic drawing of microfailure processes of hybrid short (glass/carbon) fiber-reinforced polymer composites.

lead to the final failure of the hybrid composite. As the applied strain is increased continuously, the average stress that carbon fibers bear increases. This would allow the carbon fibers to make a bigger contribution to the composite strength. Meanwhile, the glass fibers adjacent to the cracks are subjected to strain concentrations. As the applied strain is increased to  $\epsilon_5$ , the meeting of the cracks caused by the carbon fibers and by the glass fibers would lead to the final failure of the hybrid composite. Therefore, the failure strain of the hybrid composite would be higher than that of the single short carbon fiber composite but would be lower than that of the single short glass fiber composite, which has been shown in Fig. 8.

It was reported that the interfacial shear stress be-

tween the fiber and matrix in a short fiber reinforced composite increases as the applied strain is increased and the mean shear stress is proportional to the applied strain [37]. From the data of the failure strain of the composites given in Fig. 8, the values of the mean interfacial shear stress between (glass and carbon) fibers and matrix at the failure of the composites are then obtained and used in the prediction of the composite strength. Firstly, the strength of the single short fiber composites can be estimated by [14]

$$\sigma_{cu} = \chi_1 \chi_2 V_f \sigma_{fu} + V_m \sigma_m \quad (4)$$

where  $\chi_1$  and  $\chi_2$  are the fiber orientation and length factors taking into account the effects of the fiber length and orientation distributions, respectively;  $\sigma_{cu}$  and  $\sigma_{fu}$



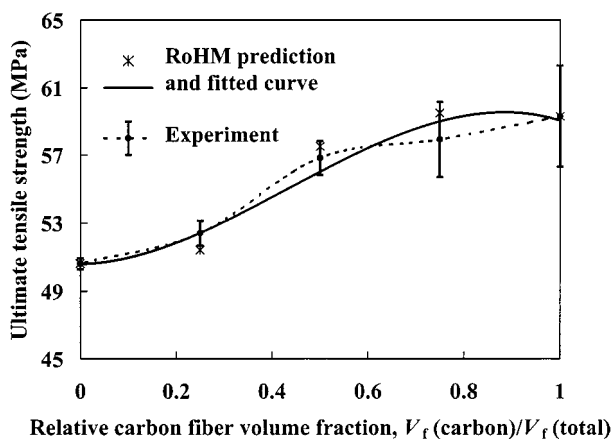


Figure 11 Quantitative explanation of the positive hybrid effect on the ultimate strength of hybrid SGF/SCF/PP composites.

are the ultimate strength of the composite and fiber, respectively;  $V_f$  and  $V_m$  denote the volume fraction of the fiber and matrix; and  $\sigma_m$  is the matrix stress at the failure of the composite.  $\chi_2$  can be assumed approximately unchanged with the relative fiber volume fraction since the fiber orientation distribution maintains roughly unchanged with relative fiber volume fraction.  $V_f = 25\%$  for both single glass and carbon fiber composites and  $V_m = 75\%$ .  $\sigma_m$  can be obtained from the stress-strain curve of the pure PP matrix [23] and the failure strain of the hybrid composites.  $\chi_2$  can be approximately estimated by for  $l_{\text{mean}} \leq l_c$

$$\chi_2 = l_{\text{mean}}/(2l_c) \quad (5)$$

where  $l_{\text{mean}}$  denotes the mean fiber length. The strength of single fiber composites is evaluated using Equations 4 and 5 by taking into consideration the variance in the interfacial shear stress (Note: this variance was not considered in the predicted results shown in Fig. 6). Then, Equation 1 can be used to estimate the strength of the hybrid composites and the predicted values of the composite strength are presented in Fig. 11. It shows that the predicted values are close to the experimental values. Since the failure strain of the hybrid composites is higher than that of the single carbon fiber composite, the mean interfacial shear stress between carbon fiber and polypropylene in the hybrid composites is higher than that in the single carbon fiber reinforced composite at failure. Thus, the carbon fibers in the hybrid composites would make a larger contribution to the composite strength than the carbon fibers do in the single carbon fiber reinforced composite. Consequently, the positive hybrid effect on the composite strength has been interpreted in a quantitative manner (Fig. 11).

#### 4. Conclusions

The tensile properties of injection molded hybrid polypropylene composites reinforced with short glass fibers and short carbon fibers have been investigated. The results have shown that the tensile strength and modulus of the hybrid composites increase with increasing relative carbon fiber volume fraction while the failure strain of the hybrid composites increases with

decreasing relative carbon fiber volume fraction. The hybrid effects have been studied on the tensile properties of the hybrid composites. A positive hybrid effect has been observed for the ultimate strength while no hybrid effect is noted for the tensile modulus. Moreover, a positive hybrid effect has been shown for the failure strain of the hybrid composites. Finally, explanations for the hybrid effects on the tensile strength and the failure strain have been presented.

#### References

1. A. R. BUNSELL and B. HARRIS, *Composites* **5** (1974) 157.
2. G. MAROM, S. FISHER, F. R. TULER and H. D. WAGNER, *J. Mater. Sci.* **13** (1978) 1419.
3. J. SUMMERSCALES and D. SHORT, *Composites* **9** (1978) 157.
4. M. M. STEVANOVIC and T. B. STECENKO, *J. Mater. Sci.* **27** (1992) 941.
5. L. N. PHILLIPS, *Composites* **7** (1976) 7.
6. M. R. PIGGOTT and B. HARRIS, *J. Mater. Sci.* **16** (1981) 687.
7. G. KRETSIS, *Composites* **18** (1987) 13.
8. I. L. KALNIN, in *Composite Materials: Testing and Design* (Second Conference), ASTM STP 497 (ASTM, February, 1972) p. 551.
9. H. FUKUDA, *J. Mater. Sci.* **19** (1983) 974.
10. C. ZWEBEN, *ibid.* **12** (1977) 1325.
11. M. MIWA and N. HORIBA, *ibid.* **29** (1994) 973.
12. *Idem.*, *ibid.* **28** (1993) 6741.
13. X. ZHU, Z. LI, Y. JIN and W. J. D. SHAW, *Compos. Sci. Technol.* **50** (1994) 431.
14. S. Y. FU and B. LAUKE, *ibid.* **56** (1996) 1179.
15. M. G. BADER and J. F. COLLINS, *Fibre Sci. Technol.* **18** (1983) 217.
16. L. BIOLZI, L. CASTELLANI and I. PITACCO, *J. Mater. Sci.* **29** (1994) 2507.
17. P. T. CURTIS, M. G. BADER and J. E. BAILEY, *ibid.* **13** (1978) 377.
18. K. FRIEDRICH, *Compos. Sci. Technol.* **22** (1985) 43.
19. S. Y. FU and B. LAUKE, *Composites Part A* **29A** (1998) 631.
20. *Idem.*, *ibid.* **29A** (1998) 575.
21. *Idem.*, *J. Mater. Sci. Technol.* **13** (1997) 389.
22. S. Y. FU, B. LAUKE, E. MÄDER, X. HU and C. Y. YUE, *J. Mater. Process. Technol.* **89-90** (1999) 501.
23. *Idem.*, *Composites Part A* **31A** (2000) 1117.
24. P. J. HINE, R. A. DUCKETT and I. M. WARD, *Composites* **24** (1993) 643.
25. S. Y. FU, X. HU and C. Y. YUE, *Mater. Sci. Res. Intern.* **5** (1999) 74.
26. F. RAMSTEINER, *Composites* **12** (1981) 65.
27. K. TAKAHASHI and N. S. CHOI, *J. Mater. Sci.* **26** (1991) 4648.
28. E. MÄDER, K. GRUNDKE, H. J. JACOBASCH and G. WACHINGER, *Composites* **25** (1994) 739.
29. CH. MAROTZKE, *Compos. Interf.* **1** (1993) 153.
30. J. SINGLETARY, B. LAUKE, W. BECKERT and K. FRIEDRICH, *Mech. Compos. Mater. Struct.* **4** (1997) 95.
31. W. BECKERT and B. LAUKE, *Compos. Sci. Technol.* **57** (1997) 1689.
32. N. SATO, T. KURAUCHI, S. SATO and O. KAMIGAITO, *J. Mater. Sci.* **26** (1991) 3891.
33. S. Y. FU, C. Y. YUE, X. HU and Y.-W. MAI, *Compos. Sci. Technol.* **60** (2000) 3001.
34. H. L. COX, *Brit. J. Appl. Phys.* **3** (1952) 72.
35. S. Y. FU and B. LAUKE, *Comp. Sci. Technol.* **58** (1998) 389.
36. N. SATO, T. KURAUCHI, S. SATO and O. KAMIGAITO, *J. Mater. Sci.* **19** (1984) 1145.
37. R. K. MITTAL and V. B. GUPTA, *ibid.* **17** (1982) 3179.

Received 4 February  
and accepted 17 July 2000